Conf-940524--6

LA-UR- 94-1650

Title: **A Maximum-Likelihood Reconstruction Algorithm for Tomographic Gamma-Ray Nondestructive Assay**

Author(s): T. H. Prettyman, R. J. Estep, R. A. Cole, and G. A. Sheppard

Submitted to: 1994 Symposium on Radiation Measurements and Applications
The University of Michigan
Ann Arbor, MI
May 16-19, 1994
(FULL PAPER)

Los Alamos
NATIONAL LABORATORY

A MAXIMUM-LIKELIHOOD RECONSTRUCTION ALGORITHM FOR TOMOGRAPHIC GAMMA-RAY NONDESTRUCTIVE ASSAY

T. H. Prettyman, R. A. Cole, R. J. Estep, and G. A. Sheppard
Los Alamos National Laboratory, Los Alamos, NM 87545

Submitted to: 1994 Symposium on Radiation Measurements and Applications
8th in a Series
The University of Michigan
Ann Arbor, Michigan
May 16-19, 1994
(Full paper, Log #275)

A MAXIMUM-LIKELIHOOD RECONSTRUCTION ALGORITHM FOR TOMOGRAPHIC GAMMA-RAY NONDESTRUCTIVE ASSAY*

T. H. Prettyman, R. A. Cole, R. J. Estep, and G. A. Sheppard
Los Alamos National Laboratory, Los Alamos, NM 87545

A new tomographic reconstruction algorithm for nondestructive assay with high-resolution gamma-ray spectroscopy (HRGS) is presented. The reconstruction problem is formulated using a maximum-likelihood approach in which the statistical structure of both the gross and continuum measurements used to determine the full-energy response in HRGS is precisely modeled. An accelerated expectation-maximization algorithm is used to determine the optimal solution. The algorithm is applied to safeguards and environmental assays of large samples (for example, 55-gal. drums) in which high continuum levels caused by Compton scattering are routinely encountered. Details of the implementation of the algorithm and a comparative study of the algorithm's performance are presented.

INTRODUCTION

High-resolution gamma-ray spectroscopy (HRGS) is used routinely in passive gamma-ray assays of nuclear materials and radioactive waste. HRGS provides the capability to identify radionuclides from complex gamma-ray spectra and to accurately determine the full-energy response of selected gamma rays using continuum subtraction techniques. Gamma-ray nondestructive assay (NDA) instruments, such as the segmented gamma-ray scanner (SGS) and the tomographic gamma-ray scanner (TGS), use the full-energy response to determine the quantity of gamma-ray emitting material within a sample. [1,2]

*This work is supported by the US Department of Energy, Office of Safeguards and Security.

In the assay of large samples such as 55-gal. drums containing medium and high-density matrices (> 0.5 g/cm^3), continuum buildup caused by Compton scattering in the sample can substantially reduce the signal-to-noise ratio of the full-energy measurement. Signal quality is also influenced by the quantity and location of gamma-ray emitting material. For assays of low-level and transuranic (TRU) waste, the total full-energy response can vary over several orders of magnitude.

With NDA instruments that use transmission-corrected, emission-computerized tomography (ECT), such as the TGS, the wide range of measurement conditions encountered in practical applications presents a significant challenge for both the physical design of the scanner and the selection of analysis techniques. In particular, emission reconstruction algorithms that are available off-the-shelf have been found to perform poorly when the target radionuclide is present in small quantities and when the signal-to-noise ratio is low. These algorithms are valid when the full-energy measurements are obtained with high precision. However, because they do not accurately model the statistical structure of the measurements, they misbehave at low count-rates and when the continuum level is large enough to influence the statistical structure of the full-energy response.

To resolve this problem, we developed a tomographic reconstruction algorithm that precisely models the statistical structure in the full-energy response determined by HRGS. A maximum-likelihood approach was used to formulate the reconstruction problem, in which both the emission image and the expected continuum level were treated as unknowns. An expectation-maximization algorithm was developed to determine the optimal solution. The performance of the algorithm was evaluated using simulated TGS measurements.

CONTINUUM SUBTRACTION MODEL

Continuum subtraction for a single full-energy peak is usually accomplished by setting up a region of interest (ROI) around the full-energy peak and one or more ROIs in the surrounding continuum. If the shape of the continuum is known, the relationship between the measured counts in the continuum ROIs and the expected continuum counts in the peak ROI can be determined. In a simple model that is valid for continuum ROIs that are symmetric, the average number of counts per channel in the background ROIs is assumed to be equal to the average continuum counts per channel in the peak ROI (Fig. 1). For this model, the number of net counts in the peak ROI is given by

$$net = m - cb$$

where m is the gross counts in the peak ROI, b is the sum of the counts in the continuum ROIs, and c is the ratio of the number of peak ROI channels to the number of background ROI channels. The symmetric ROI model is accurate to within a few percent for a wide range of peak-to-continuum ratios and is used routinely in assays of samples containing special nuclear material [3].

In gamma-ray assays, the full-energy interaction rate within the detector is used to determine the amount of emitting material within the sample [3]. To determine the number of full-energy interactions, *FEI*, in the detector from the net counts, a correction must be made for rate loss. Assuming the true time for each measurement is the same, the number of full-energy interactions is given by

$$FEI = CF(RL) \bullet net \tag{1}$$

where *CF(RL)* is a correction factor for counting rate losses due to pile-up events and the dead time of the analog-to-digital converter. Several established techniques for determining *CF(RL)* are outlined by Parker [3]. In TGS scans where the acquisition time for each measurement can be small (~600 ms/measurement), live-time estimates provided by the MCA are inadequate because they are not updated frequently. Presently, a rate-loss source is used to determine the *CF(RL)*. For assays of ^{239}Pu, a ^{109}Cd source that emits a strong line at 88 keV is used. Rate-loss corrections using ^{109}Cd have been found to be accurate to within 1% of the useful range of gamma rays emitted by ^{239}Pu (129 to 414 keV).

EMISSION MODEL AND DATA

In both SGS and TGS assays, full-energy measurements are made for a set of scan positions defined by a scanning protocol. For a scanning protocol with *M* scan positions, the measured data set can be expressed in vector form as

$$\mathbf{m} = \left(m_1, \ldots, m_j, \ldots, m_M\right)^T$$

$$\mathbf{b} = \left(b_1, \ldots, b_j, \ldots, b_M\right)^T$$

$$\mathbf{CF(RL)} = \left[CF(RL)_1, \ldots, CF(RL)_i, \ldots, CF(RL)_M\right]^T$$

where **m** is a vector of gross counts in the peak ROI, **b** is a vector of continuum ROI counts, and **CF(RL)** is a vector of correction factors for rate loss. Equation 1 is used to determine an *FEI* value for each measurement.

With the symmetric ROI model, the relationship between the spatial distribution of emitting material within the sample and the full-energy measurements is given by

$$\mathbf{A}^{(M\mathrm{x}N)}\mathbf{x}^{(N)} = \mathbf{CF(RL)} \cdot \left[\mathbf{m}^{(M)} - c\mathbf{b}^{(M)}\right] \qquad (2)$$

where **x** is a positive vector of length N containing the image parameters that describe the distribution of emitting material within the sample and **A** is an M x N weight matrix that depends on the scanning protocol, measurement geometry, and the distribution of gamma-ray attenuating material within the sample. For tomographic reconstructions, **A** is usually large and sparse with a structure that depends on the intrinsic spatial resolution of the scanner and the scanning protocol.

RECONSTRUCTION ALGORITHM DEVELOPMENT

The objective of the tomographic reconstruction algorithm is to determine the image parameters from the measurements by solving Eq. 2 subject to a positivity constraint. Conventional reconstruction algorithms, such as constrained least-squares and algebraic reconstruction techniques (ART), account for both the positivity constraint and the fact that **A** is large, sparse, and ill-conditioned. However, because these algorithms do not model the error structure of the measurements, they perform poorly when the signal-to-noise ratio (net counts divided by continuum counts) is low and are unable to quantify activity or mass when the radionuclide is present at low levels.

To resolve this problem, we developed a maximum-likelihood algorithm that precisely models the statistical structure in the gross and continuum measurements used to determine the full-energy response. To formulate the problem, both the continuum ROI counts, **b**, and the peak ROI counts, **m**, were assumed to be Poisson variates. As a result, the likelihood function describing the probability of observing a set of measurements (**m**,**b**) given their mean values $(\overline{\mathbf{m}}, \overline{\mathbf{b}})$ is given by

$$P\left(\mathbf{m}, \mathbf{b} \middle| \overline{\mathbf{m}}, \overline{\mathbf{b}}\right) = \prod_{j=1}^{M} \frac{e^{-\overline{m}_j}\, \overline{m}_j^{\,m_j}}{m_j!} \bullet \frac{e^{-\overline{b}_j}\, \overline{b}_j^{\,b_j}}{b_j!} \tag{3}$$

Because the correction factor for rate loss is usually determined with high precision (<1%), the statistical variations in rate loss can be ignored and the mean number of counts in the peak ROI can be written as

$$\overline{\mathbf{m}} = \tilde{\mathbf{A}}\overline{\mathbf{x}} + c\overline{\mathbf{b}}$$

where

$$\tilde{\mathbf{a}}_{\mathbf{j}} = \frac{\mathbf{a}_{\mathbf{j}}}{CF(RL)_J} \qquad J = 1,\ldots,M$$

and $\mathbf{a_j}$ is the **j**th row of **A**.

The most probable mean values $(\overline{\mathbf{x}}, \overline{\mathbf{b}})$ can be determined from the measurements by maximizing the likelihood function given by Eq.3 subject to positivity constraints on the solution vectors. This leads to the following convex, nonlinear optimization problem written in terms of the log-likelihood:

<u>Problem A</u>

$$\text{minimize} \quad -\ln P = -\sum_{j=1}^{M}\left[m_j \ln\left(\mathbf{a}_{\mathbf{j}}^{\mathbf{T}} \bullet \mathbf{x} + c\bar{b}_j\right) - \mathbf{a}_{\mathbf{j}}^{\mathbf{T}} \bullet \mathbf{x} + b_j \ln \bar{b}_j - (c+1)\bar{b}_j\right]$$

$$\text{subject to} \quad \left(\mathbf{x}, \overline{\mathbf{b}}\right) > 0$$

We developed an expectation maximization algorithm to solve Problem A. Expectation maximization is an iterative for solving maximum likelihood problems that is routinely used in medical applications of ECT [4,5]. The expectation maximization approach was selected because it is robust and easy to implement and accelerate. The basic algorithm is stated without proof:

<u>Algorithm MLEM-B</u>

$$x_j^{k+1} = x_j^k \left(\sum_{i=1}^{M} \tilde{a}_{ij} \right)^{-1} \sum_{i=1}^{M} \frac{m_i \tilde{a}_{ij}}{\tilde{\mathbf{a}}_{\mathbf{i}}^{\mathbf{T}} \bullet \mathbf{x}^k + c\bar{b}_i^k} \qquad \text{for } j = 1,\ldots,N$$

$$\bar{b}_j^{k+1} = \frac{1}{c+1}\left[b_j + \frac{c m_j \bar{b}_j^k}{\tilde{\mathbf{a}}_{\mathbf{j}}^{\mathbf{T}} \bullet \mathbf{x}^k + c\bar{b}_j^k} \right] \qquad \text{for } j = 1,\ldots,M$$

$$\mathbf{x}^0, \bar{\mathbf{b}}^0 > 0$$

where **x** and **b** are the solution vectors and k is the iteration number. The solution vector **b** is an estimate of the mean continuum counts, and hence approximates **b**. It can be shown that the Algorithm MLEM-B converges to the solution of Problem A as $k \to \infty$.

IMPLEMENTATION AND NUMERICAL ACCELERATION

The algorithm was implemented in Fortran 77 on a Sparcstation 10 and in C on a Microway I-860 array processor. Following Kaufman [6], a relaxation technique employing a line-search was used to accelerate the scalar version of the algorithm. A typical optimization history for both the accelerated and unaccelerated case is shown in Fig. 2. The accelerated algorithm was found to result in a gain in speed over the unaccelerated case by more than a factor of 2. With acceleration, roughly 2 seconds are required for each iteration on the Sparcstation 10. Because our primary interest is quantification, the algorithm stopping criterion is based on the convergence of the total amount of emitting material within the sample, rather than the log-likelihood. In the accelerated case, acceptable convergence in the total amount (or mass) was routinely observed for fewer than 200 iterations, resulting in run-times averaging less than 7 minutes.

PERFORMANCE FOR QUANTIFICATION

TGS assays of a 55-gal. drum containing weapon's grade (WG) plutonium embedded in a dense matrix were used to assess the performance of the algorithm. Tomographic gamma-ray scanning was developed by the Los Alamos Nuclear Safeguards program to provide an advanced correction for bias caused by heterogeneities in the distribution of emitting and attenuating materials within large samples [1,7,8,9,10]. A substantial reduction in bias for assays of special nuclear material in 55-gal. drums has been achieved using an experimental TGS [9]. A prototype TGS has been developed and is currently being used as a platform for safeguards research. The construction of a mobile TGS for measurements of low-level and TRU waste is underway.

A typical TGS includes an isotopic transmission source that emits multiple gamma rays (for example, ^{75}Se for assays of WG plutonium) and a high-resolution spectroscopy system. A scanning protocol, in which the sample is rotated and translated continuously, is used to scan the sample at discrete elevations. Measurements of transmissions at several energies are used to determine three-dimensional images of the sample's attenuation coefficient at the assay energies. The images are used to correct for matrix attenuation in the reconstruction of the distribution of gamma rays emitted at the selected assay energies. The total amount of emitting material within the sample volume or selected sub-volume is determined by integrating the emission distribution over the volume and dividing the result by a calibration constant.

In TGS assays, the drum is divided into 15 axial layers, approximately 2.5-in. thick. Each layer is divided into roughly 100 volumes. The spatial resolution of the scanner is on the order of 2.5 in. A finite-elements approach is used to model the sample geometry. On the order of 1600 image parameters *(N=1600)* are used to describe the distribution of emitting material over the sample volume.

The scan of a layer is divided into 150 measurement intervals, each interval lasting approximately 600 ms, while the MCA is active. At the end of each interval, the ROI data needed to determine peak areas for the transmission and emission gamma rays are downloaded from the MCA. In a single-pass assay of a 55-gal. drum, 2250 measurements *(M=2250)* are made in roughly 20 minutes. The control and acquisition systems are precisely synchronized to eliminate systematic errors in interval length and position.

ROI data from an experimental passive TGS assay of a point-source of WG plutonium in a polyethylene matrix are shown in Fig 2. Note that the continuum ROI counts for the 345-keV gamma ray tend to vary with the gross and net counts. The variation is caused by the Compton continuum produced by the 414-keV line. The effect of source self-attenuation, and the presence of the continuum produced by the higher energy line, reduced the signal-to-noise ratio for the 345-keV measurement.

To assess the effect of high-continuum levels on tomographic assays, repeated TGS assays of point and distributed sources of WG plutonium were simulated using the TCNDA code system [2]. The signal quality was determined by the total net counts, a quantity that is directly proportional to source intensity, and the continuum level as measured by the percentage of total gross counts in the continuum underlying the full-energy peak. The Poisson structure in the ROI data was precisely modeled.

Simulated ROI data for a typical measurement of a point source of WG plutonium in a medium-density, heterogeneous matrix are shown in Fig. 4. With 1000 net counts and an 80% continuum level, the signal quality is poor. Note that the continuum ROI signal has a component that is proportional to the primary signal, indicating the presence of higher-energy gamma rays (for example, ^{137}Cs in the proximity of the plutonium point source).

The emission distribution was reconstructed using algorithm MLEM-B. Note that the fitted gross counts, **Ax** + *c***b**, and background counts, *c***b**, follow the "measured" quantities closely. The fitted net count signature, given by **Ax**, is noise-free and matches the signature expected for the modeled emission distribution.

In Fig. 5, bias, as measured by the ratio of the assay result to the true value, is plotted as a function of total net counts for simulated assays of WG plutonium in a medium-density, heterogeneous matrix for a continuum level of 80%. Each point is the average of 50 repeated assays. The error bars indicate the standard deviation in the distribution of the ratio. MLEM-B yields accurate assays for both point and distributed sources over the full range of net-counts.

Two competing algorithms were used to analyze the same data set. Large biases were observed for ART for assays with low total net counts. MLEM without background fitting (MLEM-FB in Fig. 5), a technique suggested by Lange and Carson [4], was also found to produce a systematic bias with low signal levels. In this approach, the mean continuum vector, $\bar{\mathbf{b}}$, is taken to be the measured vector, **b**, and only the image parameters, **x** are determined in the reconstruction. With both techniques, the bias was observed to diminish as signal quality improved.

DISCUSSION

To better understand the effect of measurement quality on algorithm performance, we examined the distribution of mean net counts predicted by the statistical models used in the formulation of several algorithms. Because the net count signal is drectly related to the emission distribution (Equation 2), the behavior of the distribution of mean net counts predicted for a single measurement should provide insight into algorithm performance. A typical set of distributions if shown in Fig. 6 for an example in which the 10 counts were observed in the peak ROI (m=10) and 2 counts were observed in the continuum ROIs

(b=2). The constant for cintinuum subtraction, c, was 2. An estimate of the net counts is m-cb=10-2x2=6.

The true distribution of mean net counts is given by the convolution of the Poisson distributions describing the mean gross and continuum counts. In the example, the distribution is broad and asymmetric (Fig. 6). Note that the most probable mean net count value is less than 6. The shape and width of the distribution was found to be sensitive to the value of the continuum subtraction constant. The distribution represents the statistical model used in the formulation of algorithm MLEM-B.

In contrast, the distribution of mean net counts given by the statistical model underlying the formulation of algorithm MLEM-FB is given by the convolution of the Poisson distribution describing the gross counts and a Dirac delta function that describes the selection of the a fixed continuum level. In the example, the distribution differs substantially from the true distribution of mean net counts. According to this model, low mean net count values are improbable. As a result, mass values tend to be biased high when the quality of the measurements is poor as observed in Fig. 5.

In reconstruction techniques such as ART and filtered back-projection (FBP) the distribution of mean net counts is single valued. In ART, statistical variations in the measurements are mapped into the null-space of **A**, resulting in image artifacts. In solutions to over-determined problems with positivity constraints, inconsistencies between the emission model and the net count data is due to measurement statistics are not resolved. This causes in significant bias in total mass even in cases where the net counts are obtained with good precision (Fig. 2).

In least-squares techniques, the underlying statistical model for mean net counts is Gaussian with a standard deviation given by $\sigma = \sqrt{m^2 + c^2 b^2}$. In the example, the Gaussian model provides a better fit to the true distribution than the model used in MLEM-FB; however, the symmetry of the Gaussian results in a right-shift in the distribution of mean counts. Because asymmetries in the distribution are not modeled, use of the least-squares techniques is expected to result in bias similar to that observed for MLEM-FB. The magnitude of the bias depends on the number of observed counts and the choice of the continuum subtraction constant.

CONCLUSIONS AND FUTURE WORK

The results of the performance study show that the continuum-fitting MLEM algorithm (MLEM-B) is capable of quantifying the total amount of emitting material for a wide range of signal qualities. The algorithm accurately models the statistical of the measurements for a specific continuum subtraction model. As a result, the performance of the algorithm for quantification is independent of the model parameters. The algorithm out-performs conventional algorithms that do not model the Poisson statistical structure in the measurements. Use of the algorithm is expected to significantly reduce quantification limits for emission tomographic scanners used for safeguards and radioactive waste assay.

Future work will focus on developing the algorithm to work with more general continuum subtraction models. Straight-line and smoothed-step models are currently being evaluated for asymmetric ROIs. For these models, each continuum ROI must be fitted independently, resulting in a minor increase in computational effort.

REFERENCES

1. R. J. Estep, "Assay of Heterogeneous Radioactive Wastes by Low-Resolution Tomographic Gamma Scanning," *Trans. Am. Nucl. Soc.*, **62** 178 (1990).

2. T. H. Prettyman, R. J. Estep, and G. A. Sheppard, "Development of a Tomographic Instrument for Gamma-Ray Nondestructive Assay," *Trans. Am. Nucl.* Soc., **69** 182-184 (1993).

3. J. L. Parker, "General Topics in Passive Gamma-Ray Assay," pp. 95-158 in Reilly, Ensslin, Smith, and Kreiher Eds., *Passive Nondestructive Assay of Nuclear Materials*, NUREG/CR-5550 (1991).

4. K. Lange and R. Carson, "EM Reconstruction Algorithms for Emission and Transmission Tomography," *Journal of Computer Assisted Tomography*, **8**:(2), 306-316 (1984).

5. L. A. Shepp and Y. Vardi, "Maximum Likelihood Reconstruction for Emission Tomography," *IEEE Transactions on Medical Imaging*, **MI-1**, No. 2, 113-122 (1982).

6. L. Kaufman, "Implementing and Accelerating the EM Algorithm for Positron Emission Tomography," *IEEE Transactions on Medical Imaging*, **MI-6**, No. 1, 37-51 (1987).

7. R. J. Estep, K. Sherwood, "A Prototype Tomographic Gamma Scanner for Assaying 208-Liter Drums," Los Alamos National Laboratory document LA-UR-91-61 (1991).

8. R. J. Estep, "TGS-FIT: Image Reconstruction Software for Quantitative, Low-Resolution Tomographic Assays," Los Alamos National Laboratory report LA-12497-MS (January 1993).

9. R. J. Estep, T. H. Prettyman, and G. A. Sheppard, "Tomographic Gamma Scanning (TGS) to Measure Inhomogeneous Nuclear Material Matrices from Future Fuel Cycles," Los Alamos National Laboratory document LA-UR-93-1637 (1993).

10. R. J. Estep, "A Preliminary Design Study for Improving Performance in Tomographic Assays," Los Alamos National Laboratory report LA-12727-MS (March 1994).

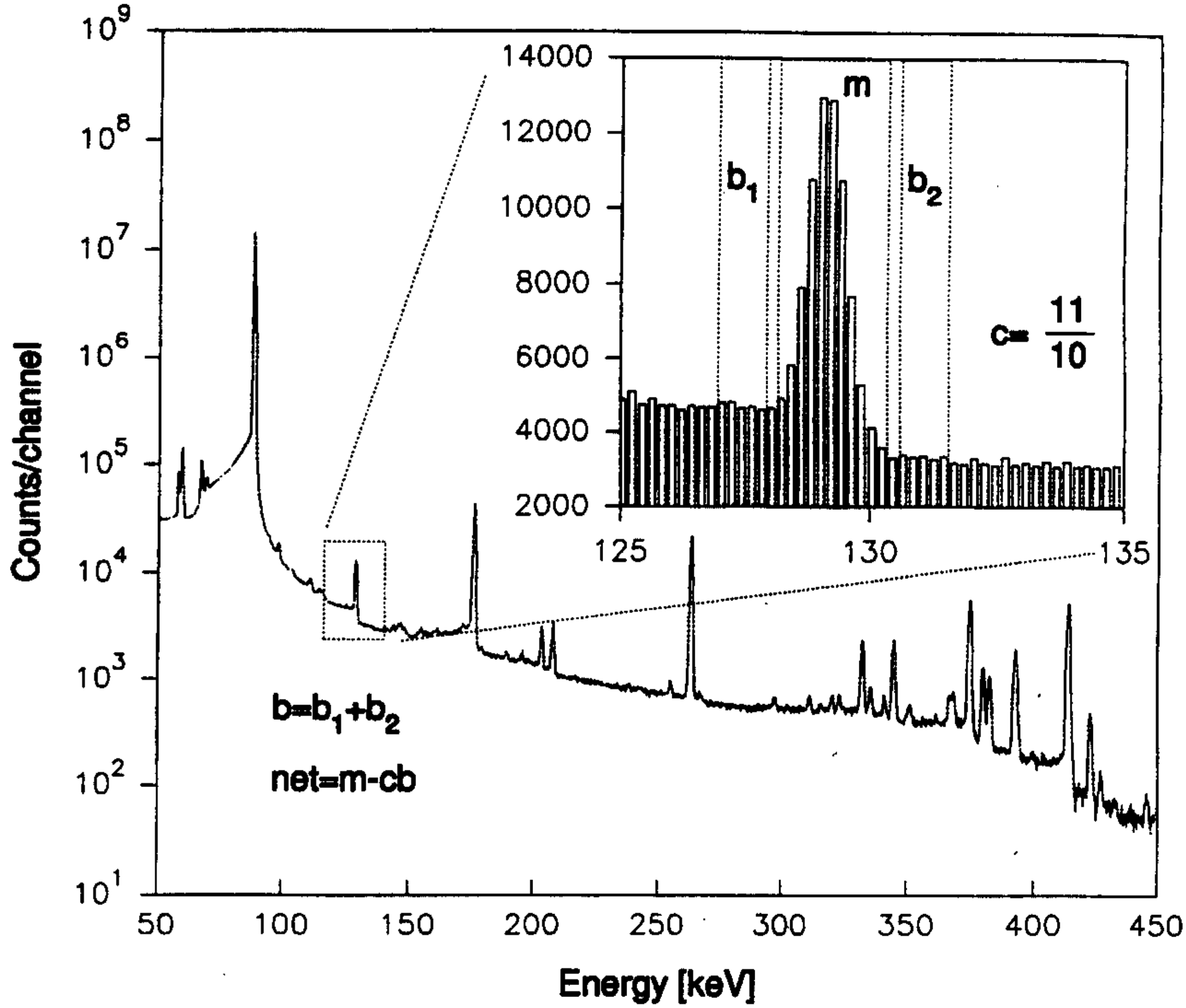

Fig. 1. An HRGS spectrum for a high-burnup plutonium source in a 55-gal. drum containing a medium-density matrix. Symmetric ROIs for continuum subtraction are shown in the exploded view for the 129-keV gamma ray emitted by ^{239}Pu.

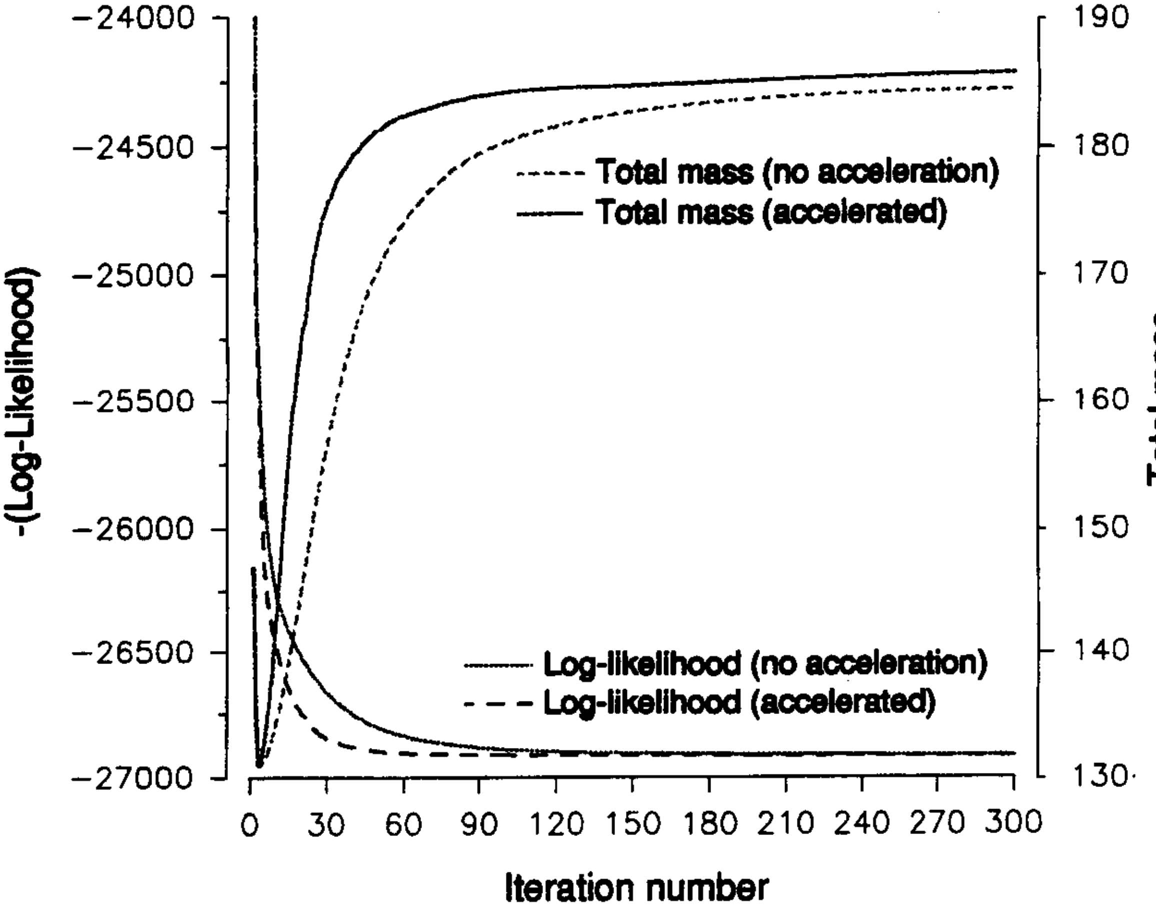

Fig. 2. Optimization histories with and without acceleration for a typical TGS reconstruction.

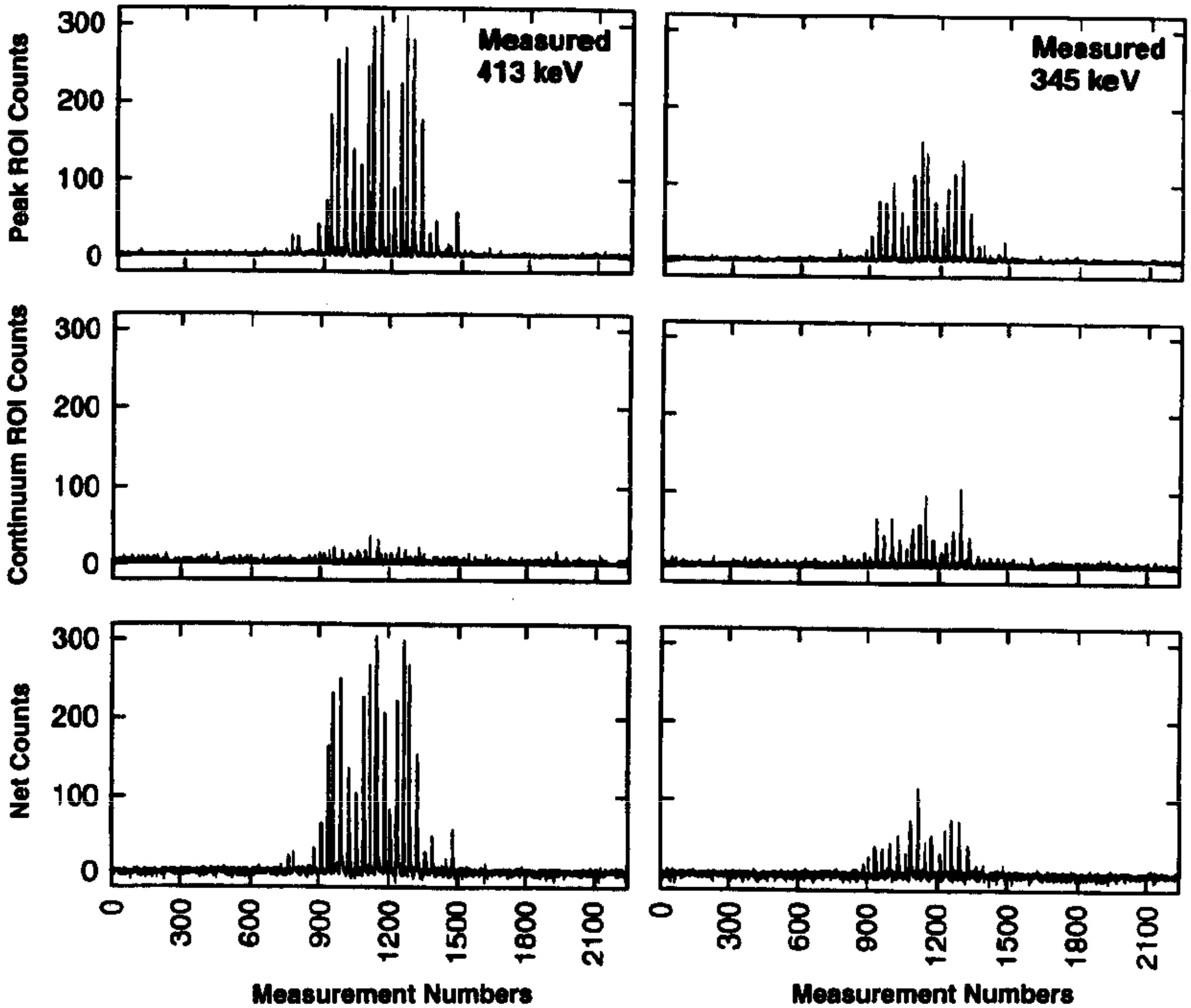

Fig. 3. Experimental TGS data for a medium density, low-Z matrix (0.6 g/cm³ polyethylene beads) containing 3 g of high-burnup plutonium. Each measurement number uniquely corresponds to a scan-position (angle, displacement, elevation) determined by the scanning protocol.[2]

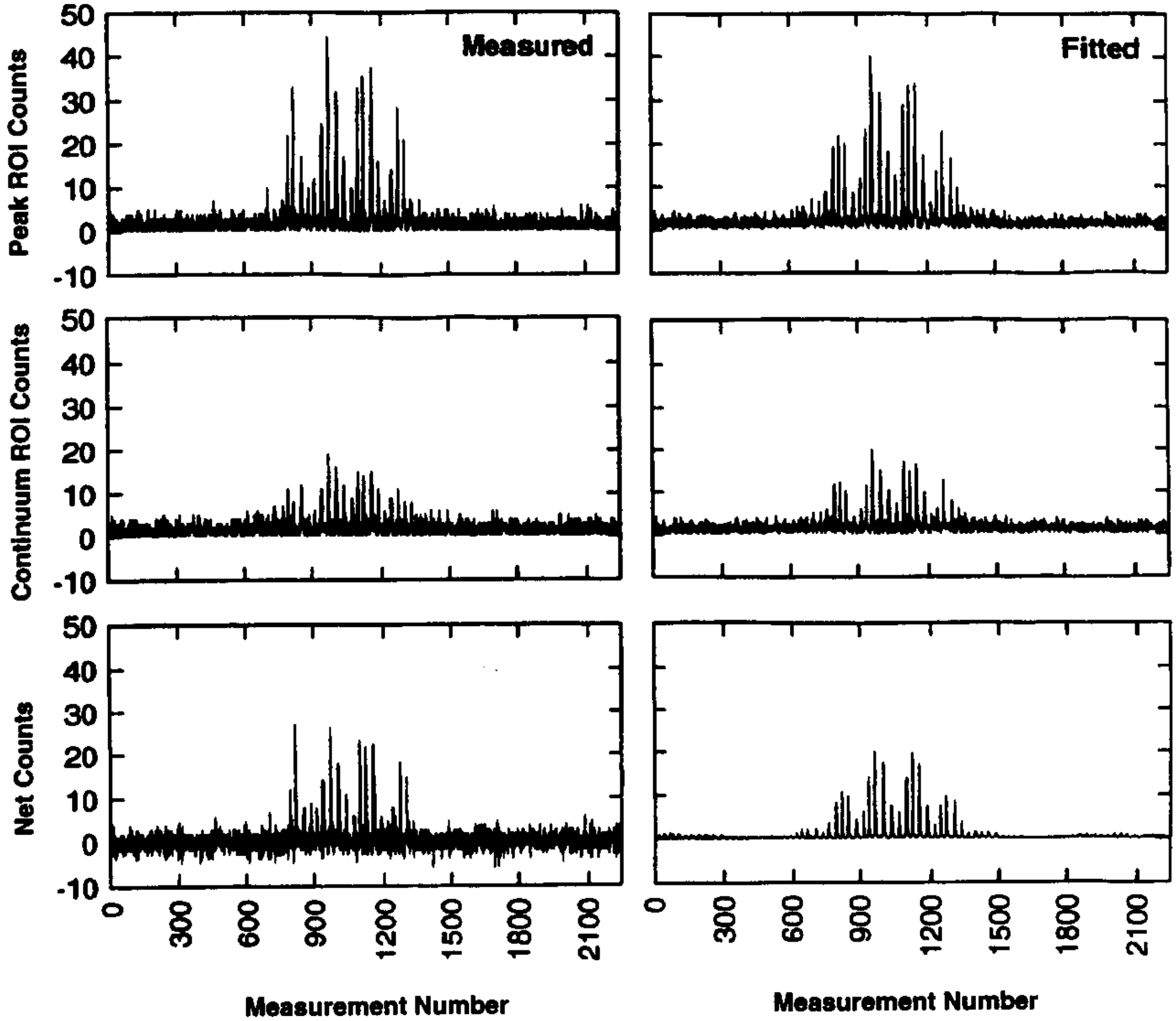

Fig. 4. Comparison between simulated and fitted TGS data for a high-continuum, low-count-rate case.

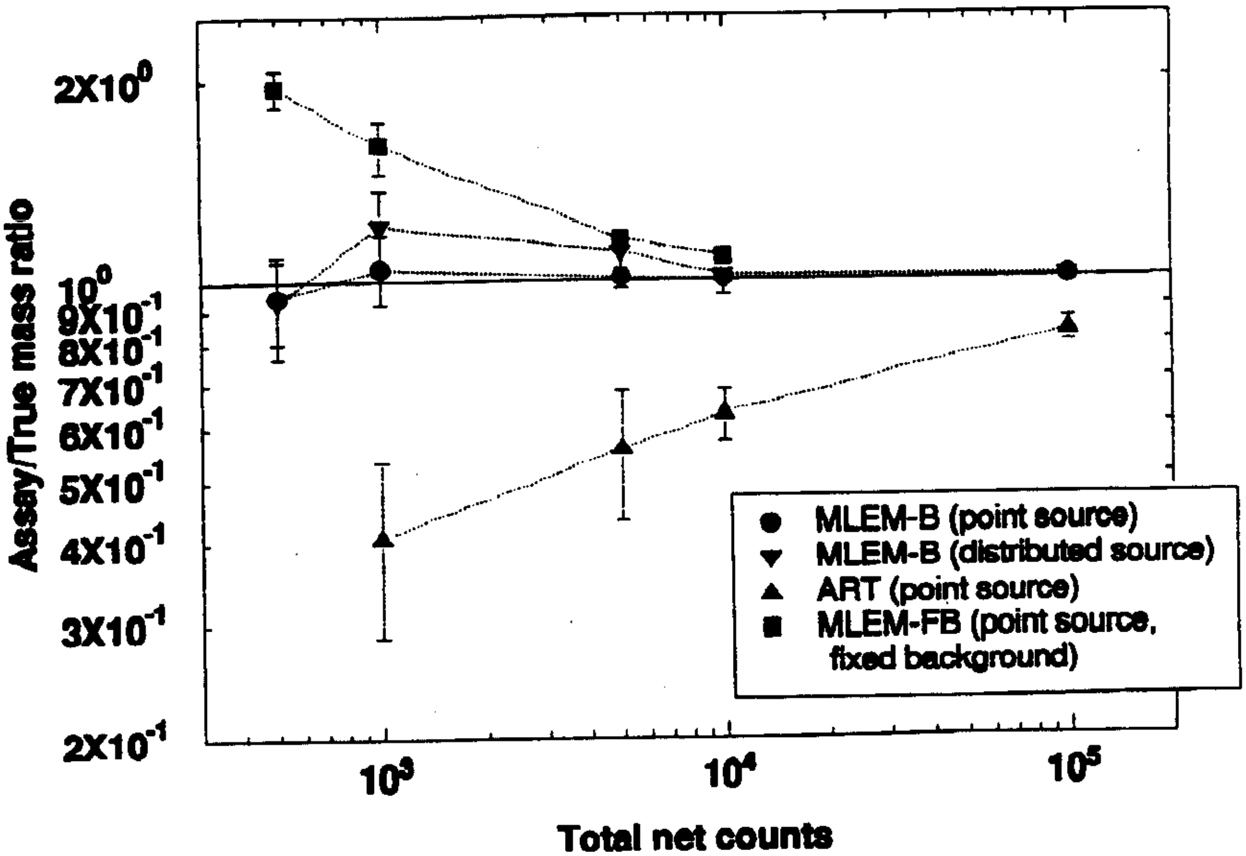

Fig. 5. Bias for various reconstruction algorithms as a function of total net counts for a fixed continuum level of 80%.

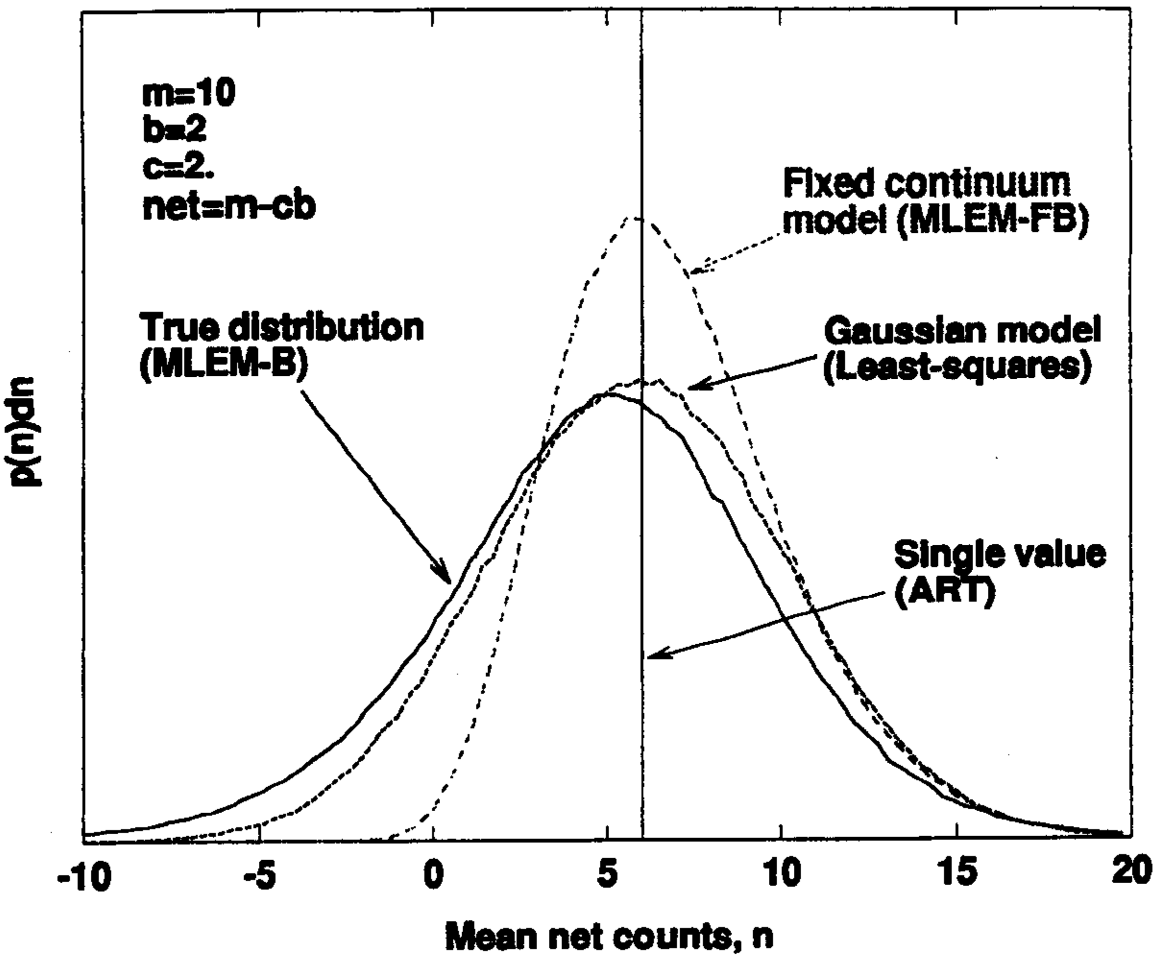

Fig. 6. The distribution of mean net counts for several models of the statistical structure of the full-energy measurements.